IJSRM
INTERNATIONAL JOURNAL OF SCIENCE AND RESEARCH METHODOLOGY
An Official Publication of Human Journals

Human Journals
Research Article
October 2022 Vol.:22, Issue:4

Mobility of Al, Fe, Mn, Ti, and Organic Matter in Xingu River Sediments

IJSRM
INTERNATIONAL JOURNAL OF SCIENCE AND RESEARCH METHODOLOGY
An Official Publication of Human Journals

Maurício Araújo de Lima*[1], Simone de Fátima Pinheiro Pereira[2, 3], Kellen Heloizy Garcia de Freitas[2, 4], Pedro Moreira de Sousa Junior[2, 5], Cléber Silva e Silva[2, 6], Alan Marcel Fernandes de Souza[6], Renan Arruda da Costa[2]

[1] Technology Center for Power Plants in Northern Brazil (ELETRONORTE) Arthur Bernardes Highway, 2172 - Telégrafo, Belém - PA- Brazil. [2]Environmental and Analytical Chemistry Laboratory, Federal University of Pará. Augusto Correa Street, S/N - Guamá, Belém - PA - Brazil. [3]Chemistry Postgraduate Program, Federal University of Pará. Augusto Correa Street, S/N - Guamá, Belém - PA - Brazil. [4]Faculty of Materials Engineering, Federal University of Pará Ananindeua Campus. We Twenty-six Street, 2 - Coqueiro, Ananindeua - PA- Brazil. [5]Federal Rural University of the Amazon. Barão de Capanema Avenue S/N - Caixa D'Água, Capanema - PA - Brazil. [6]Federal Institute of Education, Science, and Technology of Pará. Almirante Barroso Avenue, 1155 - Marco, Belém - PA - Brazil.

Submitted: 25 September 2022
Accepted: 30 September 2022
Published: 30 October 2022

Keywords: sediments, Brazilian amazon, geochemical environment, lithology

ABSTRACT

The objective of this work was to evaluate the mobility of Al, Fe, Mn, Ti, and organic matter in the sediments of the area called Volta Grande do Xingu, the site is influenced by the Belo Monte Hydroelectric Complex, municipality of Altamira-Pará, region of Brazilian Amazon. In relation to the total content of elements found in the sediments, the order of abundance obtained, based on the average found in the analyzed points, was: Al (20560 $mg.kg^{-1}$) > Fe (16148 $mg.kg^{-1}$) > Ti (5534 $mg.kg^{-1}$) > Mn (273 $mg.kg^{-1}$). As for the distribution of elements in the geochemical environment, the mobility order found was: Mn (50.8%) > Fe (1.53%) > Al (0.60%) > Ti (0.00%). The organic matter contents ranged from 0.73 to 19.73%, with an average value of 4.95±4.48%. The data obtained revealed a high association between Fe-Mn-Ti, mainly attributed to the lithology of the region.

HUMAN JOURNALS
www.ijsrm.humanjournals.com

INTRODUCTION

Chemical elements participate in the aquatic environment in several processes that can result in alteration of their physicochemical properties (speciation) or their spatial distribution (migration), thus affecting their availability to aquatic organisms [1,2]. Some of these processes only occur at very low concentrations of the participating element, where it tends to adsorb on the surface of solid particles of low adsorption capacity dispersed in the aqueous system or compact solid phases in contact with the system, such as surfaces of vessels and utensils used in the handling and analysis of water samples [3].

The dynamics of chemical elements are more complex in rivers than in lakes and oceans. This is because, in all aquatic systems, the behavior of the material present in it is associated with the movement of water [4]. However, in rivers, this becomes even more pronounced, as they constitute systems that present a large amount of allochthonous material (dissolved and in suspension) being transported by their waters [5].

The Xingu River is part of the Amazon River Basin and is one of the largest tributaries of the Amazon River, where the Negro rivers are on the left bank; the Uatumã; Paru and on the right bank, the Purus; the Madeira; the Tapajós and the Iriri-Xingu [6]. The regime of its waters is controlled by the rainfall in the basin region, where the alternation of rainy periods to the south and the north guarantees a permanent supply of the Amazon River throughout the year, causing the fluctuations in the levels of its waters to present a much smaller amplitude. than would occur if it were subjected to a single rainfall regime [7,8].

Within the Amazonian context, the Xingu River and its main tributary, the Iriri, is classified as clear water river, its transparency and greenish color being remarkable, showing a low content of suspended materials [6,9]. The clear water rivers that are born in the Cretaceous sediments deposited above the shield of Central Brazil are acidic, extremely poor in mineral salts, and with low concentrations of calcium and magnesium [10]. As for the concentration of humic substances, it is higher at the beginning of the rainy season, when the first rains transport humic material accumulated in the soils during the dry season to the rivers [11]. Therefore, at the beginning of the rainy season, its waters may appear turbid due to a large amount of suspended material [12].

The Xingu River basin crosses two important Brazilian ecosystems: the Cerrado and the Amazon rainforest. Therefore, the topography of the region has a significant influence on its vegetation, which will determine the physicochemical characteristics of the floodplains and solid ground [13,14]. On dry land, the presence of water is conditioned by rainfall, and atmospheric humidity, where leaching takes place with greater or lesser intensity according to the permeability of the soils [15]. In the sedimentation floodplains, the telluric water is constant and contributes to the enrichment of the soil. In the igapó floodplains, the waters are almost devoid of sediment and have an erosive action, determining a continuous lowering of the soil, increasingly deepening the flooded area [16].

The presence of major and trace elements in the environment is associated with rock weathering and human activities [17]. When available in the environment, these chemical species can travel through a series of aquatic systems, being retained in compartments, such as sediments, or being remobilized [18]. Sediments are particles derived from rocks or biological materials that can be found at the bottom of rivers, lakes, and oceans, among others. In aquatic systems, organic matter from animals and plants that have not been fully decomposed and chemical elements can be retained in these geochemical compartments, stored in significant quantities, which come from marine and terrestrial sources - in addition to these, toxic elements and pesticides can also be incorporated into sediments [19].

These chemical species interact with various geochemical supports present in the sediments, through mechanisms such as adsorption, complexation, coprecipitation, diffusion processes, and biological absorption, and exhibit different binding mechanisms with carbonates, oxides, and hydroxides of Fe and Mn, organic matter, sulfides and with constituents of refractory crystalline minerals, such as silicates [20,21]. In this way, these geochemical compartments play an important role in the temporary fixation of these elements and the subsequent transport of many chemical compounds, that is, promoting their mobility [22].

It is possible to verify that the mobility of the major elements is mainly related to environmental and geochemical changes at the water-sediment interface, such as pH, salinity, and presence of organic matter [23]. In general, if there is oxidation in the medium and a decrease in pH, there is an increase in the solubility of the elements; if the system undergoes a reduction and an increase

in pH, stable organo-mineral complexes can be formed. As for salinity, it is seen that the increase in salinity causes the solubility of the compounds since the metal ions tend to have low ionic activity, involving mobility. Finally, two other important salinity factors are the association of metal ions with chlorine and competition for sorption surfaces with Na, K, Ca, and Mg cations, which are abundant in waters with higher salinity [24].

It is important to highlight that sediments are also responsible for the pollution of aquatic systems, such as rivers, by toxic elements, since they act as a source of these contaminants. These compounds tend to be deposited in sediments together with organic matter, Fe and Mn oxides and hydroxides, and sulfides and are associated with finer particles such as clay [25]. Whenever there are changes in the environment and in the geochemistry at the water-sediment interface, which is subjected to several biotic and abiotic processes, such as alteration of the hydrogenation potential, presence of organic chelators, or amount of organic matter, the sediments can end up releasing these metals, thus promoting their re-disposition in the water and their transfer to other parts of the aquatic system [26]. In this way, these compartments can be used to detect, track and monitor the presence of contaminants, being extremely important for studies of impacts on the environment [27,28].

The objective of this work was to determine the contents of Al, Fe, Ti, and Mn elements and of organic matter in sediments from the Volta Grande region of the Xingu River, to evaluate the mobility of these elements at the water-sediment interface, as well as their association. with organic matter.

METHODOLOGY

Study area

The work area is located in the central portion of the State of Pará, limited to the north and south by parallels 3°00' and 4°00' S, respectively; to the east by the meridian 51°00' WGr and to the west by the meridian 52°30' WGr, covering part of the municipalities of Altamira, Senador José Porfírio and Portel (Figure 1).

The region under study is known as the Volta Grande of the Xingu River, a stretch with numerous waterfalls and rapids. The tributaries of the right bank of the Xingu River, among

which the Ituna, Itatá, Bacajá, and Anapu rivers stand out, present intense mining activity in their course, especially in the vicinity of the Três Palmeiras mountain range [29]. Table 1 lists the collection points and the local geology.

Collection and pre-treatment of sediment samples

Sampling was carried out with a boat using a Van Venn dredger and global positioning system (GPS) to georeference the points collected along the area called Volta Grande of the Xingu River. There were a total of 34 points, the samples being identified and preserved under refrigeration in polyethylene packages until their pre-treatment. The collection regions were divided into groups according to specific criteria regarding local geochemistry:

Table 2 summarizes the collection regions.

After collecting the samples, they were packed in polyethylene packages and kept refrigerated at 4 ºC until they were properly treated. Then they were dried in an oven at a temperature of 60 °C for 24 hours. After drying, the samples were homogenized (200 mesh) and digested in the microwave. For the total decomposition of samples, the sample heating system by microwave radiation DGT 100 from Provecto was used.

Approximately 0.25 g of sediment was weighed in each reactor, and then 3 mL of HF, 9 mL of HNO_3, 2 mL of HCl, and 1 mL of H_2O_2 were added, and a blank was prepared for every 10 samples. The hydrogen peroxide had to be added slowly to prevent over-reaction that could cause the sample to overflow from the reactor flask. Then, the samples were submitted to the following heating steps: 8 minutes at a power of 250 W; 4 minutes at 400 W; 6 minutes at 600 W; and 2 minutes at 0 W. The system was then cooled for 1 hour in an ice bath and then 2 mL of 100 $g.L^{-1}$ H_3BO_3 solution was added and the samples were submitted to the following heating step: 3 minutes at 300 W; 2 minutes at 0 W. This step aims to complex the residual hydrofluoric acid to prevent it from reacting with instrumental components sensitive to this acid (quartz torch, nebulizer, nebulization chamber). The solutions resulting from this procedure were then measured in a 50 mL flask for further elemental analysis. All water used had a minimum resistivity of 18.2 $M\Omega.cm^{-1}$ and was supplied by Elga's Purelab ultra analytic purification system, which used distilled water as a feed.

Sequential extraction

The distribution of metals in sediment fractions was determined by sequential extraction proposed by the Tests, Measurements, and Standards Program of the European Union (SM&T) and consists of three successive extractions that allow us to associate the metals with one of the following phases: soluble phase in acid, reducible phase, oxidizable phase, residual or inert phase. The sequential extraction procedure used is described below.

Acid-soluble phase (fraction 1): Initially, 1 g of the sample was weighed in a polyethylene centrifuge tube with a capacity of 50 mL, and 40 mL of 0.11 M acetic acid was added. The system was stirred for 16 hours and then the supernatant is separated from the solid residue by centrifugation. Then, the residue was washed with 20 mL of ultrapure water and subjected again to agitation for another 15 minutes and to centrifugation for 15 minutes.

Reducible phase (fraction 2): 40 mL of 0.5 M hydrochlorination hydroxylamine was added to the residue obtained in fraction 1 and stirred for 16 hours. Centrifugation was performed to separate the supernatant. Then, the residue obtained was washed as described above.

Oxidizable phase (fraction 3): In this step, 25 mL of 30 % concentrated H_2O_2 was added to the residue of the fraction and then heated in a water bath for 1 h at 85 ºC until the volume was reduced. This procedure was repeated three more times, totaling 20 mL of H_2O_2 used. After cooling the tube, 50 mL of 1.0 M ammonium acetate was added, the system being shaken and washed as described in the fraction 2 step. Residual or inert phase (fraction 4): In this step, the total digestion of the residue is obtained by completing the sequential extraction procedure.

Metal analysis

For the simultaneous determination of the elements (Al, Fe, Mn, and Ti), a Varian inductively coupled plasma optical emission spectrometer (ICP-OES) Vista Pro was used with axial configuration, equipped with a 40 MHz radio frequency and a sample introduction system consisting of concentric nebulizer and cyclonic nebulization chamber (Varian, Australia). Analytical results were validated through accuracy and precision studies using standard sediment reference material analysis.

Organic carbon determination

The determination of the organic carbon content (% C) was carried out by titrating the excess dichromate in an acidic medium with a solution of $Fe(NH_4)_2(SO_4)_2$ [30]. The percentage of organic matter (% OM) can be obtained by multiplying the percentage of organic carbon by the factor of 1.725. This factor is used because it is assumed that in the average composition of humus, carbon participates with 58% [31].

The following procedure was used for the determination of organic carbon according to the methodology of [32]. 0.5 g of the sediment (dried and pulverized) was transferred to a 250 mL Erlenmeyer flask. 20 mL of concentrated sulfuric acid and 10 mL of 1 N potassium dichromate were added, with the Erlenmeyer flask being gently shaken. It was left to rest for 30 minutes. After this time, 200 mL of deionized water and 10 mL of concentrated phosphoric acid were added. A 0.5 N solution of $Fe(NH_4)_2(SO_4)_2$ was used as the titrant solution and 1 % diphenylamine as an indicator.

RESULTS AND DISCUSSION

Total metals and organic matter content in Xingu River sediments

The results obtained for the total concentrations of the selected metals presented the following order of abundance for the elements Al > Fe > Ti > Mn; which evidences the dominant characteristics in the chemical composition of these collected sediments, since they are, respectively, the 3rd (after silicon and oxygen), 4th, 9th and 12th most abundant element in the continental terrestrial crust [33].

In the separation by groups (Table 3), the abundance remained the same (Al > Fe > Ti > Mn) for the Xingu I, Xingu II and Xingu V groups. There was a change in the abundance in the Xingu III groups (Fe > Al > Ti > Mn) and Xingu IV (Fe > Ti > Al > Mn), where the Fe element was the most abundant.

The variability of the results of the evaluated elements and organic matter is shown in Figure 2.

Al had its average total concentration of 20560±13984 $mg.kg^{-1}$, ranging from 4564 $mg.kg^{-1}$ at point SSX35 to 83752 $mg.kg^{-1}$ at point SSX08. Al presented greater variation in its results in the

Xingu I group, with an anomalous result (SSX08). Two anomalous Al results were also found in the Xingu III group (SSX27 and SSX28) which comprises the area close to the mining, with strong anthropic influence. An anomalous result was found for Al at point SSX10 (Gaioso channel).

As it is a major component of clay minerals in the Xingu River, human activities and even the seasonal period may have led to high variability in the concentration of the element, which is compatible with its content in the most common aluminosilicate mixtures found in the region, such as kaolinite and illite [34]. Al, even in high concentrations, does not cause damage to organisms residing in sediments and has no limited value in sediment quality lists [35]. Fe showed a total average content of 16148±14419 $mg.kg^{-1}$, ranging from 3797 $mg.kg^{-1}$ at point SSX07 and 88213 $mg.kg^{-1}$ at point SSX35.

The Fe contents, whose concentration is on the threshold between the values that do not cause damage to organisms residing in sediments (TEC - threshold effect concentration), are below 20,000 $mg.kg^{-1}$, a value above the average found in this work, however lower than the values found in points SSX28, SSX29, SSX30, points of the Xingu III group close to the mines, with strong anthropic influence [35].

The highest Fe content (SSX35) and with the highest variability appeared in the Xingu IV group, points close to Belo Monte with a strong influence of vehicle transport and also close to the city of Vitória do Xingu without anomalous results. Fe was concentrated in the sediments of environments richer in laterites. Fe is a component of clay minerals, replacing in certain situations Mg^{2+} (ionic radius similar to Fe^{2+}) or as a component of specific minerals, such as hematite or goethite [36,37].

Less dominant among the elements is Mn, with a general average of 273±244 $mg.kg^{-1}$ whose contents ranged from 59.9 $mg.kg^{-1}$ at point SSX07 to 1387 $mg.kg^{-1}$ at point SSX35. The greatest variability of results for Mn was found in the Xingu IV Group, with strong anthropic influence. An anomalous result was found in the Xingu I group, at point SSX08, which corresponds to a point close to the island of Taboca. The TEC value for Mn is 460 $mg.kg^{-1}$, three points showed Mn concentration values above this limit, SSX08 point in the Xingu River near Taboca Island, SSX28 point near the Garimpo do Galo grotto, both with 1.4 times above the TEC and the

SSX35 point on the Xingu River near Belo Monte with a grade three times above. These results reinforce the anthropic influence that occurs in the Xingu III and IV groups, in addition to the SSX08 point near Taboca Island.

Ti showed a mean total concentration of 5534±12308 $mg.kg^{-1}$, ranging from 1132 $mg.kg^{-1}$ at point SSX07 to 74354 $mg.kg^{-1}$ at point SSX35. Ti showed practically no variability in its results, except for the Xingu IV Group, with strong anthropic influence. Again, point SSX35 appears with high values of chemical elements attributed to the presence of roads, farms, and banks without vegetation cover. Ti is an element with little mobility and both Mn and Ti can participate in the crystalline lattice of clay minerals [38,39]. Ti, like Al, has no limit between the values that do not cause damage to sediment-resident organisms.

The levels of organic matter found in the sediments on the banks of the Xingu River ranged from 0.73 to 19.73%, with an average value of 4.95% and a standard deviation of 4.48%, indicating that organic matter, in the places studied, originates from diffuse sources along the Xingu River and reveals the influence of the dominant characteristics of the degradation of organic, natural and anthropic matter in this environment.

In sediments, the elements are mainly complex with organic matter [40]. As for the limnological classification, the sediments of the Xingu River can be classified as inorganic and organic sediments, where samples SSX33, SSX25, SSX10, and SSX09 presented values of organic matter above 10 % of their dry weight [41]. These high values are probably due to the human influence existing both in the Xingu River and in its tributaries. These receive loads of urban effluents since these samples were collected close to urban centers in the region, such as, for example, point SSX33, located on the Tucuruí River near the Vitória do Xingu city.

Correlation between metals and organic matter

To verify if the total concentration of metals comes from the geochemistry of the region, being part of its mineralogical constitution, a study was carried out to evaluate the correlation between the major and minor elements and the organic matter content. The results obtained are shown in Table 4. Significant correlations (Sic.) are those with $p < 0.050$.

The results obtained in the correlations show a high geochemical association between Al, Mn, and Ti, between Fe and Ti, and between Mn and Ti in the Xingu I group ($p < 0.050$), which shows the dominant characteristics of the geology of the region [29].

Sediments are from oxic, suboxic, and anoxic environments [42]. In oxic sediments, organic matter is mineralized by the action of microorganisms that use dissolved oxygen as the final electron acceptor. In suboxic sediments, nitrates and Fe and Mn oxide minerals serve as oxidizing agents for the degradation of organic matter into inorganic carbonate species. In anoxic sediments, electrons from organic matter are transferred to sulfate and bicarbonate ions, which are reduced to sulfide and methane, respectively [43].

The dissolved products of anaerobic mineralization reactions are transported by diffusion across concentration gradients in the interstitial water, therefore Mn(II) and Fe(II) can reach the oxic zone and be further oxidized by dissolved oxygen to form new mineral oxides on the surface. of the sediment [43,44].

Al does not present a significant correlation with any other element studied, which can be explained through the geology of the region, since according to [29] the mineral phases most commonly found in the region are plagioclase - $(Na,Ca)Al(Si, Al)Si_2O_8$, quartz - SiO_2 and microcline - $K(AlSi_3O_8)$, while other minerals such as biotite - $K(Mg,Fe)_3(AlSi_3O_{10})(OH)_2$ and hornblende - $Ca_2(Mg,Fe)_4Al[Si_7AlO_{22}](OH)_2$ occur in smaller amounts.

Distribution of metals in the phases of the sediments

The distribution of Al, Fe, Mn, and Ti in the sediment phases is shown in Figure 3.

For Al, a variation from 2.80 to 25.52% was found in the total concentration present in the mobile phase (acid-soluble phase, reducible phase, and oxidizable phase), with a content lower than 10% in most points, except points SSX09, SSX15, SSX23 and SSX28 to SSX36, where the most significant phases are the reducible phase and the oxidizable phase, with little importance for the acid-soluble phase.

This highlights the chemistry of Al in the aquatic environment, as it is only significantly solubilized in the water column at pH values below 4.0 (in fraction 1 the extracting solution has a pH close to 5.0). The SSX33 point was where Al showed greater mobility, with about 10% in the

reducible phase and 10% in the oxidizable phase, which indicates dominant characteristics of the geochemistry of the Tucuruí River (Alter do Chão formation).

The Fe was widely distributed in the mobile phase, mainly in the reducible fraction, with a percentage in the total mobile phase ranging from 1.64% (SSX35) to 61.75% (SSX17), with little importance for its percentages in the soluble phases. in acid and oxidizable. This is because fraction 3 corresponds to the elements bound to the oxides of Fe and Mn since these are excellent scavengers of trace metals from water and are relatively unstable in an anoxic environment [45]. The SSX35 point showed the lowest mobility, which reveals the influence of the Alter do Chão formation in the sample collected.

On the other hand, Mn presented a very different behavior, since in most points a large percentage of this element was obtained in the acid-soluble fraction, which comprises the most easily exchangeable geochemical phase, requiring only a slight change in the pH of the aqueous phase [46,47]. It is demonstrated that Mn changes its concentration mainly in winter and spring, where concentrations were relatively high compared to reference stations [48].

Among the elements evaluated, Ti was the one with the lowest mobility, with contents in the mobile phase ranging from 0.03 % to 1.25 %. This is due to the tendency of this element to remain in the aluminosilicate structures, which gives it little availability for the aqueous phase. The large accumulation of Al, Fe, and Ti in the residual phase of the sediment are probably due to the natural origin due to the influence of the geochemistry of the region, since these are among the most abundant elements in the continental earth's crust [49].

CONCLUSIONS

The order of abundance (Al > Fe > Ti > Mn) found agrees with the order suggested for these elements in the continental earth's crust. As for the mobility of the aforementioned elements, grouped according to the concentrations obtained from the acid-soluble phase (Mn > Fe > Al > Ti), it is in agreement with expectations since this phase consists of the most labile and bioavailable geochemical phase, and can therefore easily pass to the aqueous phase.

In the Volta Grande region of the Xingu River, in general, no evidence of anthropic influence on the chemical composition of the studied sediments was found. The exception is in the locations

immediately close to regions impacted by the mining activities present mainly in the tributaries of the right bank of the Xingu River (SSX28 and SSX29), including the Ituna, Itatá, Bacajá, and Anapu rivers. In these regions, the presence of gold mineralization occurs largely in the Serra das Três Palmeiras region, whose geochemistry influences most of the samples collected (SSX20 to SSX32).

ACKNOWLEDGMENT

The authors would like to thank the National Electric Energy Agency (ANEEL) for funding the Project (Nº Contract: 4500013841) and Eletronorte for supporting field and laboratory work. We would also like to thank the Laboratory of Analytical and Environmental Chemistry and the Graduate Program in Chemistry at UFPA for providing their laboratory structure and technical support for the preparation of the project.

REFERENCES

1. NAMIEŚNIK, J.; RABAJCZYK, A. The speciation and physico-chemical forms of metals in surface waters and sediments. Chemical Speciation & Bioavailability, v. 22, n. 1, p. 1-24, 2010. https://doi.org/10.3184/095422910X12632119406391

2. FERNANDES, L. L.; KESSARKAR, P. M.; RAO, V. P.; SUJA, S.; PARTHIBAN, G.; KURIAN, S. Seasonal distribution of trace metals in suspended particulate and bottom sediments of four microtidal river estuaries, west coast of India. Hydrological Sciences Journal, v. 64, n. 12, p. 1519-1534, 2019. https://doi.org/10.1080/02626667.2019.1655147

3. N'GORAN, K. P. D. A.; DIABATE, D.; KOUASSI, N'G. L. B.; YAO, K. M.; KINIMO, K. C.; OUATTARA, A. A.; TROKOUREY, A. Geochemical speciation and distribution of trace metals in sediments around industrial and artisanal gold mining areas in northern Côte d'Ivoire. Environmental Earth Sciences, v. 81, n. 333, p. 1-18, 2022. https://doi.org/10.1007/s12665-022-10447-0

4. MAKI, J. S.; HERMANSSON, M. The dynamics of surface microlayers in aquatic environments. The Biology of Particles in Aquatic Systems, ed. 2, p. 161-182, 2020.

5. MOL, P. A. S.; SUJATHA, C. H. Distribution and geochemical speciation of sediment bound heavy metals in the specific zones of central Kerala, India. Environmental Nanotechnology, Monitoring & Management, v. 14, n. 3, p. 100358, 2020. https://doi.org/10.1016/j.enmm.2020.100358

6. FRICKE, A. T.; NITTROUER, C. A.; OGSTON, A. S.; NOWACKI, D. J.; ASP, N. E.; SOUZA FILHO, P. W. M.; SILVA, M. S.; JALOWSKA, A. M. River tributaries as sediment sinks: Processes operating where the Tapajós and Xingu rivers meet the Amazon tidal river. Sedimentology, v. 64, n. 6, p. 1731-1753, 2017. https://doi.org/10.1111/sed.12372

7. CANTONATI, M.; POIKANE, S.; PRINGLE, C. M.; STEVENS, L. E.; TURAK, E.; HEINO, J.; RICHARDSON, JOHN S.; BOLPAGNI, R.; BORRINI, A.; ČTVRTLÍKOVÁ, M.; GALASSI, D. M. P.; HÁJEK, M.; HAWES, I.; LEVKOV, Z.; NASELLI-FLORES, L.; SABER, A. A.; DI CICCO, M.; FIASCA, B.; HAMILTON, P.B.; KUBEČKA, J.; SEGADELLI, S.; ZNACHOR, P. Characteristics, main impacts, and stewardship of natural and artificial freshwater environments: consequences for biodiversity conservation. Water, v. 12, n. 260, p. 1-85, 2020. https://doi.org/10.3390/w12010260

8. MORAN, E. F.; LOPEZ, M. C.; MOORE, N.; HYNDMAN, D. W. Sustainable hydropower in the 21st century. Proceedings of the National Academy of Sciences, v. 115, n. 47, p. 11891-11898, 2018. https://doi.org/10.1073/pnas.1809426115
9. MAGALHÃES, K. X.; SILVA, R. D. F.; SAWAKUCHI, A. O.; GONÇALVES, A. P.; GOMES, G. F. E.; CUNHA, J. M.; SABAJ, M. H.; SOUSA, L. M. Phylogeography of Baryancistrus xanthellus (Siluriformes: Loricariidae), a rheophilic catfish endemic to the Xingu River basin in eastern Amazonia. PloS one, v. 16, n. 8, p. e0256677, 2021. https://doi.org/10.1371/journal.pone.0256677
10. NASCIMENTO JR, D. R.; SAWAKUCHI, A. O.; GUEDES, C. C. F.; GIANNINI, P. C. F.; GROHMANN, C. H.; FERREIRA, M. P. Provenance of sands from the confluence of the Amazon and Madeira rivers based on detrital heavy minerals and luminescence of quartz and feldspar. Sedimentary Geology, v. 316, p. 1-12, 2015. https://doi.org/10.1016/j.sedgeo.2014.11.002
11. LEE, B. J.; KIM, J.; HUR, J.; CHOI, I. H.; TOORMAN, E. A.; FETTWEIS, M.; CHOI, J. W. Seasonal Dynamics of Organic Matter Composition and Its Effects on Suspended Sediment Flocculation in River Water. Water Resources Research, v. 55, n. 8, p. 6968-6985, 2019. https://doi.org/10.1029/2018WR024486
12. RIBEIRO, D. R. G.; FACCIN, H.; MOLIN, T. R. D.; CARVALHO, L. M.; AMADO, L. L. Metal and metalloid distribution in different environmental compartments of the middle Xingu River in the Amazon, Brazil. Science of the Total Environment, v. 605-606, p. 66-74, 2017. https://doi.org/10.1016/j.scitotenv.2017.06.143
13. ARRUDA, D. M.; SCHAEFER, C. E. G. R.; FONSECA, R. S.; SOLAR, R. R. C.; FERNANDES-FILHO, E. I. Vegetation cover of Brazil in the last 21 ka: New insights into the Amazonian refugia and Pleistocenic arc hypotheses. Global Ecology and Biogeography, v. 27, n. 1, p. 47-56, 2018. https://doi.org/10.1111/geb.12646
14. SCHIESARI, L.; ILHA, D. D.; NEGRI, D. D. B.; PRADO, P. I.; GRILLITSCH, B. Ponds, puddles, floodplains and dams in the Upper Xingu Basin: could we be witnessing the 'lentification'of deforested Amazonia?. Perspectives in Ecology and Conservation, v. 18, n. 2, p. 61-72, 2020. https://doi.org/10.1016/j.pecon.2020.05.001
15. SHAO, W.; NI, J.; LEUNG, A. K.; SU, Y.; WAI NG, C. W. Analysis of plant root–induced preferential flow and pore-water pressure variation by a dual-permeability model. Canadian Geotechnical Journal, v. 54, n. 11, p. 1537-1552, 2017. https://doi.org/10.1139/cgj-2016-0629
16. WOHL, E. E. Transient landscapes: insights on a changing planet. Colorado: University Press of Colorado, 2015.
17. BARZEGAR, R.; MOGHADDAM, A. A.; TZIRITIS, E.; FAKHRI, M. S.; SOLTANI, S. Identification of hydrogeochemical processes and pollution sources of groundwater resources in the Marand plain, northwest of Iran. Environmental Earth Sciences, v. 76, n. 7, p. 1-16, 2017. https://doi.org/10.1007/s12665-017-6612-y
18. MASINDI, V.; MUEDI, K. L. Environmental contamination by heavy metals. Heavy metals, v. 10, p. 115-132, 2018. https://doi.org/10.5772/intechopen.76082
19. KALEV, S. D.; TOOR, G. S. The composition of soils and sediments. Green Chemistry, p. 339-357, 2018. https://doi.org/10.1016/B978-0-12-809270-5.00014-5
20. BANDARA, T.; FRANKS, A.; XU, J.; BOLAN, N.; WANG, H.; TANG, C. Chemical and biological immobilization mechanisms of potentially toxic elements in biochar-amended soils. Critical Reviews in Environmental Science and Technology, v. 50, n. 9, p. 903-978, 2020. https://doi.org/10.1080/10643389.2019.1642832
21. SHI, M.; MIN, X.; KE, Y.; LIN, Z.; YANG, Z.; WANG, S.; PENG, N.; YAN, X.; LUO, S.; WU, J.; WEI, Y. Recent progress in understanding the mechanism of heavy metals retention by iron (oxyhydr) oxides. Science of the Total Environment, v. 752, p. 141930, 2021. https://doi.org/10.1016/j.scitotenv.2020.141930
22. CARMACK, E. C.; YAMAMOTO-KAWAI, M.; HAINE, T. W. N.; BACON, S.; BLUHM, B. A.; LIQUE, C.; MELLING, H.; POLYAKOV, I. V.; STRANEO, F.; TIMMERMANS, M.-L.; WILLIAMS, W. J. Freshwater and its role in the Arctic Marine System: Sources, disposition, storage, export, and physical and biogeochemical consequences in the Arctic and global oceans. Journal of Geophysical Research: Biogeosciences, v. 121, n. 3, p. 675-717, 2016. https://doi.org/10.1002/2015JG003140

23. DIOP, C.; OUDDANE, B. Study of the mobility of trace elements at the water-sediment interface in coastal and estuarine areas. Journal of Water Science, v. 32, n. 4, p. 463-474, 2020. https://doi.org/10.7202/1069578ar
24. LYONS, W. B.; CAREY, A. E.; GARDNER, C. B.; WELCH, S. A.; SMITH, D. F.; SZYNKIEWICZ, A.; DIAZ, M. A.; CROOT, P.; HENRY, T.; FLYNN, R. The geochemistry of Irish rivers. Journal of Hydrology: Regional Studies, v. 37, n. 100881, 2021. https://doi.org/10.1016/j.ejrh.2021.100881
25. SUN, X.; FAN, D.; LIU, M.; TIAN, Y.; PANG, Y.; LIAO, H. Source identification, geochemical normalization and influence factors of heavy metals in Yangtze River Estuary sediment. Environmental pollution, v. 241, p. 938-949, 2018. https://doi.org/10.1016/j.envpol.2018.05.050
26. DEBNATH, A.; SINGH, P. K.; SHARMA, Y. C. Metallic contamination of global river sediments and latest developments for their remediation. Journal of Environmental Management, v. 298, p. 113378, 2021. https://doi.org/10.1016/j.jenvman.2021.113378
27. GEISSEN, V.; MOL, H.; KLUMPP, E.; UMLAUF, G.; NADAL, M.; VAN DER PLOEG, M.; VAN DE ZEE, S.; RITSEMA, C. Emerging pollutants in the environment: a challenge for water resource management. International soil and water conservation research, v. 3, n. 1, p. 57-65, 2015. https://doi.org/10.1016/j.iswcr.2015.03.002
28. PETRIE, B.; BARDEN, R.; KASPRZYK-HORDERN, B. A review on emerging contaminants in wastewaters and the environment: current knowledge, understudied areas and recommendations for future monitoring. Water research, v. 72, p. 3-27, 2015. https://doi.org/10.1016/j.watres.2014.08.053
29. CPRM, Programa Levantamentos Geológicos Básicos do Brasil: Altamira - Folha SB.22-Y-D. Brasília: CPRM/DIEDIG/DEPAT, 2001.
30. BAHADORI, M.; TOFIGHI, H. A modified Walkley-Black method based on spectrophotometric procedure. Communications in Soil Science and Plant Analysis, v. 47, n. 2, p. 213-220, 2016. https://doi.org/10.1080/00103624.2015.1118118
31. UFOT, U. O.; IREN, O. B.; CHIKERE NJOKU, C. U. Effects of land use on soil physical and chemical properties in Akokwa area of Imo State, Nigeria. International Journal of Life Sciences Scientific Research, v. 2, n. 3, p. 273-278, 2016.
32. WALKLEY, A.; BLACK, A. An examination of the Degtjareff method for determining soil organic matter, and a proposed modification of the chromic acid titration method. Soil Sci., v. 37, n. 1, p. 29-38, 1933.
33. WEDEPOHL, K. H. The composition of the continental crust. Geochimica et Cosmochimica Acta, v. 59, n. 7, p. 1217-1232, 1995. https://doi.org/10.1016/0016-7037(95)00038-2
34. BERTASSOLI JR, D. J.; SAWAKUCHI, A. O.;, CHIESSI, C. M.;, SCHEFUß, E.; HARTMANN, G. A.;, HÄGGI, C.; CRUZ, F. W.; ZABEL, M.; MCGLUE, M. M.; SANTOS, R. A.; PUPIM, F. N. Spatiotemporal variations of riverine discharge within the Amazon Basin during the late Holocene coincide with extratropical temperature anomalies. Geophysical Research Letters, v. 46, n. 15, p. 9013-9022, 2019. https://doi.org/10.1029/2019GL082936
35. CAVALCANTI NETO, M. T. O.; FARIA, M. S. S.; DANTAS NETO, J.; CAVALCANTI, J. M. M. Qualidade de sedimentos - um estudo de caso na região de confluência dos rios Piranhas e Seridó no Rio Grande do Norte. Holos, n. 5, p. 151-166, 2012.
36. JENA, S. K.; SAHOO, H.; RATH, S. S.; RAO, D. S.; DAS, S. K.; DAS, B. Characterization and processing of iron ore slimes for recovery of iron values. Mineral Processing and Extractive Metallurgy Review, v. 36, n. 3, p. 174-182, 2015. https://doi.org/10.1080/08827508.2014.898300
37. LUAN, F.; LIU, Y.; GRIFFIN, A. M.; GORSKI, C. A.; BURGOS, W. D. Iron (III)-bearing clay minerals enhance bioreduction of nitrobenzene by Shewanella putrefaciens CN32. Environmental science & technology, v. 49, n. 3, p. 1418-1426, 2015. https://doi.org/10.1021/es504149y
38. KOME, G. K.; ENANG, R. K.; TABI, F. O.; YERIMA, B. P. K. Influence of clay minerals on some soil fertility attributes: a review. Open Journal of Soil Science, v. 9, n. 9, p. 155-188, 2019. https://doi.org/10.4236/ojss.2019.99010
39. VAN GROENINGEN, N.; ARRIGO, L. K. T.; BYRNE, J. M.; KAPPLER, A.; CHRISTL, I.; KRETZSCHMAR, R. Interactions of ferrous iron with clay mineral surfaces during sorption and subsequent

oxidation. Environmental Science: Processes & Impacts, v. 22, n. 6, p. 1355-1367, 2020. https://doi.org/10.1039/D0EM00063A

40. SHI, P.; SCHULIN, R. Erosion-induced losses of carbon, nitrogen, phosphorus and heavy metals from agricultural soils of contrasting organic matter management. Science of the Total Environment, v. 618, p. 210-218, 2018. https://doi.org/10.1016/j.scitotenv.2017.11.060

41. SAWAKUCHI, A. O.; HARTMANN, G. A.; SAWAKUCHI, H. O.; PUPIM, F. N.; BERTASSOLI, D. J.; PARRA, M.; ANTINO, J. L.; SOUSA, L. M.; PEREZ, M. H. S.; OLIVEIRA, P. E.; SANTOS, R. A.; SAVIAN, J. F.; GROHMANN, C. H.; MEDEIROS, V. B.; MCGLUE, M. M.; BICUDO, D. C.; FAUSTINO, S. B. The Volta Grande do Xingu: reconstruction of past environments and forecasting of future scenarios of a unique Amazonian fluvial landscape. Scientific Drilling, v. 20, p. 21-32, 2015. https://doi.org/10.5194/sd-20-21-2015

42. YUAN, W.; LIU, G.; STEBBINS, A.; XU, L.; NIU, X.; LUO, W.; LI, C. Reconstruction of redox conditions during deposition of organic-rich shales of the Upper Triassic Yanchang Formation, Ordos Basin, China. Palaeogeography, Palaeoclimatology, Palaeoecology, v. 486, p. 158-170, 2017. https://doi.org/10.1016/j.palaeo.2016.12.020

43. OLDHAM, V. E.; SIEBECKER, M. G.; JONES, M. R. ; MUCCI, A.; TEBO, B. M.; LUTHER III, G. W. The Speciation and Mobility of Mn and Fe in Estuarine Sediments. Aquatic Geochemistry, v. 25, p. 3-26, 2019. https://doi.org/10.1007/s10498-019-09351-0

44. RASSMANN, J.; EITEL, E. M.; LANSARD, B.; CATHALOT, C.; BRANDILY, C.; TAILLEFERT, M.; RABOUILLE, C. Benthic alkalinity and dissolved inorganic carbon fluxes in the Rhône River prodelta generated by decoupled aerobic and anaerobic processes, Biogeosciences, v. 17, p. 13–33, 2020. https://doi.org/10.5194/bg-17-13-2020, 2020

45. OLUBODUN, S. O.; ERIYAMREMU, G. E. Spatial Distribution and Chemical Fractionation of Some Heavy Metals in Crude Oil Spill Soil. BIU Journal of Basic and Applied Sciences, v. 3, n. 1, p. 10-19, 2017.

46. CRUZ-HERNÁNDEZ, Y.; RUIZ-GARCÍA, M.; VILLALOBOS, M.; ROMERO, F. M.; MEZA-FIGUEROA, D.; GARRIDO, F.; HERNÁNDEZ-ALVAREZ, E.; PI-PUIG, T. Fractionation and mobility of thallium in areas impacted by mining-metallurgical activities: identification of a water-soluble Tl (I) fraction. Environmental Pollution, v. 237, p. 154-165, 2018. https://doi.org/10.1016/j.envpol.2018.02.031

47. XU, X.; HUANG, R.; LIU, J.; SHU, Y. Fractionation and release of Cd, Cu, Pb, Mn, and Zn from historically contaminated river sediment in Southern China: Effect of time and pH. Environmental toxicology and chemistry, v. 38, n. 2, p. 464-473, 2018. https://doi.org/10.1002/etc.4330

48. BERRADA, M.; EL HMAIDI, A.; MONYR, N.; ABRID, D.; ABDALLAOUI, A.; ESSAHLAOUI, A.; EL OUALI, A. Self-organizing map for the detection of seasonal variations in Sidi Chahed Dam sediments (Northern Morocco). Hydrological Sciences Journal, v. 61, n. 3, p.628-635, 2016. http://dx.doi.org/10.1080/02626667.2014.964717

49. SOW, M. A.; PAYRE-SUC, V.; JULIEN, F.; CAMARA, M.; BAQUE, D.; PROBST, A.; SIDIBE, K.; PROBST, J. L. Geochemical composition of fluvial sediments in the Milo River basin (Guinea): is there any impact of artisanal mining and of a big African city, Kankan?. Journal of African Earth Sciences, v. 145, p. 102-114, 2018. https://doi.org/10.1016/j.jafrearsci.2018.05.009

50. CPRM/DNPM, Folha de Altamira (SA.22-Y-D), projeto Altamira - Programa grande Carajás Mapeamento geológico, integrado ao projeto especial de mapas de recurso minerais, CPRM/DNPM, Projeto Integração Geológico-Geofísica Sul do Pará, 1979.

51. CPRM/DNPM, Projeto Norte da Amazônia Domínio Oiapoque-Jarí, Geologia da folha AS-22Y vol. IV Ministério de Minas e Energia convênio CPRM/DNPN Companhia de Pesquisa de Recursos Minerais - Diretoria de Operações, agência de Belém, 1974.

52. SIOLE, H. Alguns Resultados e Problemas da Limnologia Amazônica. Bol. Técnico do Instituto Agrônomo do Norte, Belém-PA, p. 24, 1951.

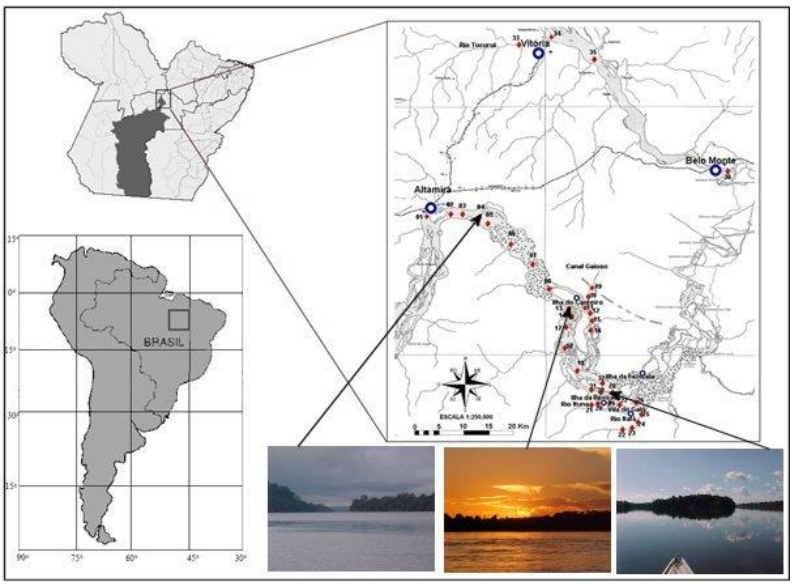

Figure 1. Location map of sampling points

Source: Adapted from [50,51].

Table 1. **Relationship between the geology of the studied area and the collection points**

Collection points	**Geological formation**
SSX01	Devonian - Ererê formation[1]
SSX02	Sinéclisis type basin: Ererê formation*,[1]
SSX03	Sinéclisis type basin: Maecuru formation *,[1]
SSX04	Sineclisis type basin: Trombetas group*,[1]
SSX05 a SSX21, 25 a 32 e 36	Polycyclically Thickened Sialic Crust Area (Xingu Metamorphic Suite)[1]
SSX22 a 24, 26 e 27	Greenstone Belt (Tres Palmeiras metamorphic suite)*,[1]
SSX33 a 35	Amazon Sedimentary Basin: Tertiary Coverage of Barreiras Formation [2]

*Alluvial Influence; [1][50]; [2][52].

Table 2. Division of the collections regions

Collection region	Collection points	Local description
Xingu I	SSX02 to 08	Portion of the Xingu River between the city of Altamira and Ilha da Taboca.
Xingu II	SSX12 to 19	Portion of the river Xingu between Ilha Máster and Ilha Borges (points of interest due to the proximity of the Belo Monte HPP, Pimental site).
Xingu III	SSX26 to 32	Between Ilha do Vieira and Ilha do Eloi, points of interest due to the proximity of Garimpos.
Xingu IV	SSX34 to 36	Points near the Belo Monte HPP, between Fazenda do Danilo and Corredeira Island, closer to the city of Vitória do Xingu downstream of the Pimental Site.
Xingu V	SSX01 (Panelas); SSX09-11 (Gaioso); SSX20-21 (Ituna); SSX22-25 (Itatá); SSX33 (Tucuruí)	This group comprises some tributaries of the Xingu River.

Table 3. Descriptive statistics of the results of elements and Organic Matter in sediment (mg.kg^{-1})

Descriptive Statistics	Xingu I					Descriptive Statistics	Xingu II				
	Al	**Fe**	**Mn**	**Ti**	**OM[1]**		**Al**	**Fe**	**Mn**	**Ti**	**OM[1]**
Mean	**32750**	12225	254	2079	2,95	Mean	23472	11338	153	2359	3,79
Median	25404	11687	168	1957	2,00	Median	24673	11847	135	2531	3,60
SD[2]	27127	5381	219	862	2,40	SD[2]	7600	3680	65,8	566	3,14
Minimum	7254	3797	59.9	1132	1.30	Minimum	8135	4464	82.3	1293	0.70
Maximum	83752	19158	660	3409	7.70	Maximum	31145	16569	283	2974	9.70
Descriptive Statistics	Xingu III					Descriptive Statistics	Xingu IV				
	Al	**Fe**	**Mn**	**Ti**	**OM[1]**		**Al**	**Fe**	**Mn**	**Ti**	**OM[1]**
Mean	17087	21578	283	3005	3.90	Mean	6154	**37472**	**635**	**28490**	2.27
Median	15897	18635	181	3110	2.80	Median	4870	12908	378	8370	1.30
SD[2]	5622	9808	191	694	2.90	SD[2]	2493	43951	662	39818	1.67
Minimum	11633	10644	109	2086	0.70	Minimum	4564	11294	140	2748	1.30
Maximum	29295	38105	628	4041	9.00	Maximum	9027	88213	1387	74354	4.20
Descriptive Statistics	Xingu V										
	Al	**Fe**	**Mn**	**Ti**	**OM[1]**						
Mean	17668	12153	265	5031	**8.59**						
Median	16125	11411	259	4428	7.55						
SD[2]	6813	4385	102	2076	5.91						
Minimum	10293	6717	60.5	3671	1.70						
Maximum	33949	19221	448	10759	19.70						

[1]OM= Organic Matter (%); [2]SD= Standard Deviation

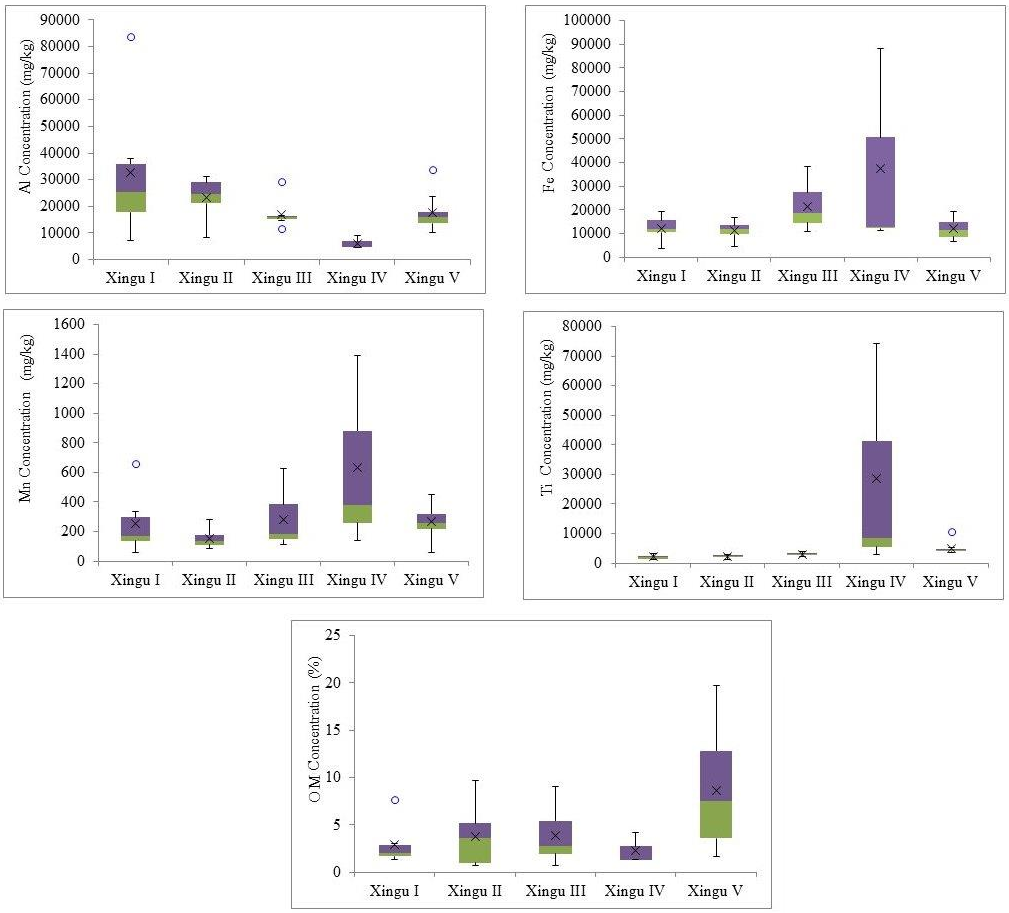

Figure 2. Variability of the elements Al, Fe, Mn, Ti (mg.kg^{-1}) and Organic Matter (%) in sediments

OM= Organic Matter

Table 4. Correlation between elements and Organic Matter in sediments

Elements/ OM[1]	Xingu I					Elements/ OM[1]	Xingu II				
	Al	**Fe**	**Mn**	**Ti**	**OM[1]**		**Al**	**Fe**	**Mn**	**Ti**	**OM[1]**
Al	1.000					**Al**	1.000				
Sic.[2]	-					**Sic.[2]**	-				
Fe	0.718	1.000				**Fe**	0.493	1.000			
Sic.[2]	0.108	p= -				**Sic.[2]**	0.215	-			
Mn	**0.993**	0.740	1.000			**Mn**	0.115	0.537	1.000		
Sic.[2]	**0.000**	0.093	-			**Sic.[2]**	0.787	0.170	-		
Ti	**0.939**	**0.834**	**0.932**	1.000		**Ti**	**0.711**	0.645	-0.128	1.000	
Sic.[2]	**0.005**	**0.039**	**0.007**	-		**Sic.[2]**	**0.048**	0.084	0.763	-	
OM[1]	-0.019	0.590	0.049	0.168	1.000	**OM[1]**	-0.021	0.281	**0.827**	-0.285	1.000
Sic.[2]	0.972	0.218	0.927	0.751	-	**Sic.[2]**	0.960	0.501	**0.011**	0.494	-
Elements/ OM[1]	**Xingu III**					**Elements/ OM[1]**	**Xingu IV**				
	Al	**Fe**	**Mn**	**Ti**	**OM[1]**		**Al**	**Fe**	**Mn**	**Ti**	**OM[1]**
Al	1.000					**Al**	1.000				
Sic.[2]	-					**Sic.[2]**	-				
Fe	**0.795**	1.000				**Fe**	-0.567	1.000			
Sic.[2]	**0.033**	-				**Sic.[2]**	0.616	-			
Mn	**0.787**	**0.977**	1.000			**Mn**	-0.693	0.987	1.000		
Sic.[2]	**0.036**	**0.000**	-			**Sic.[2]**	0.513	0.103	-		
Ti	0.375	0.690	0.549	1.000		**Ti**	-0.610	**0.999**	0.994	1.000	
Sic.[2]	0.407	0.086	0.202	-		**Sic.[2]**	0.583	**0.033**	0.070	-	
OM[1]	-0.416	-0.145	-0.217	0.277	1.000	**OM[1]**	**0.998**	-0.516	-0.648	-0.560	1.000
Sic.[2]	0.354	0.757	0.641	0.547	-	**Sic.[2]**	**0.039**	0.655	0.552	0.622	-
Elements/ OM[1]	**Xingu V**										
	Al	**Fe**	**Mn**	**Ti**	**OM[1]**						
Al	1.000										
Sic.[2]	-										
Fe	0.385	1.000									
Sic.[2]	0.271	-									
Mn	-0.007	0.030	1.000								
Sic.[2]	0.985	0.935	-								
Ti	-0.006	-0.033	**0.661**	1.000							
Sic.[2]	0.986	0.928	**0.037**	-							
OM[1]	0.421	0.263	**-0.644**	-0.354	1.000						
Sic.[2]	0.226	0.463	**0.044**	0.315	-						

OM[1]= Organic Matter; **Sic.[2]** = Significant correlations; Marked p <0.050

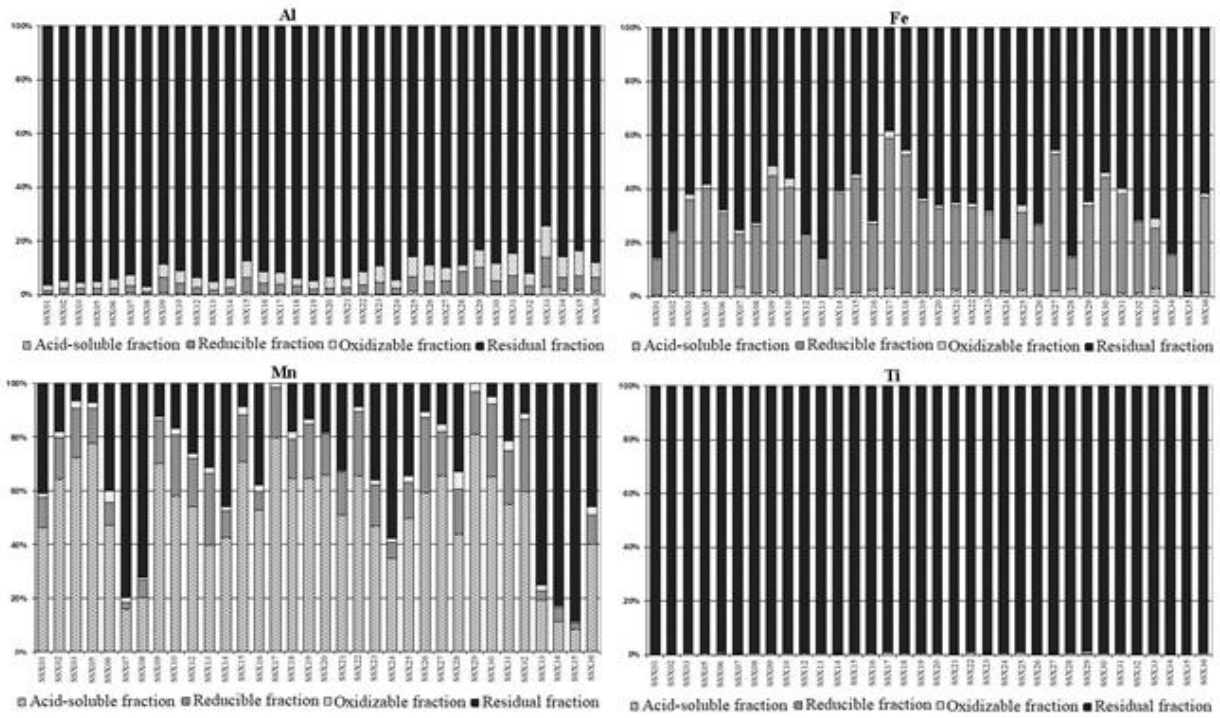

Figure 3. Distribution of Al, Fe, Mn and Ti in the sediment phases

Image Author -1	***Maurício Araújo de Lima – Corresponding Author*** *Technology Center for Power Plants in Northern Brazil (ELETRONORTE)* *Arthur Bernardes Highway, 2172 - Telégrafo, Belém - PA- Brazil*
Image Author - 2	***Simone de Fátima Pinheiro Pereira*** *Chemistry Postgraduate Program, Federal University of Pará* *Augusto Correa Street, S/N - Guamá, Belém - PA - Brazil*
Image Author - 3	***Kellen Heloizy Garcia de Freitas*** *Faculty of Materials Engineering, Federal University of Pará* *Ananindeua Campus* *WE 26, Street 2 - Coqueiro, Ananindeua - PA - Brazil*
Image	***Pedro Moreira de Sousa Junior*** *Federal Rural University of the Amazon, Capamena Campus*

Author - 4	*Barão de Capanema Avenue S/N - Caixa D'Água, Capanema - PA – Brazil*
Image Author - 5	***Cléber Silva e Silva*** *Federal Institute of Pará* *Almirante Barroso Avenue, 1155 - Marco, Belém - PA - Brazi*
Image Author - 6	***Alan Marcel Fernandes de Souza*** *Federal Institute of Pará* *Almirante Barroso Avenue, 1155 - Marco, Belém - PA - Brazi*
Image Author - 7	***Renan Arruda da Costa*** *Environmental and Analytical Chemistry Laboratory, Federal University of Pará* *Augusto Correa Street, S/N - Guamá, Belém - PA - Brazil*